Available online at www.sciencedirect.com
SCIENCE DIRECT®
Journal of Sound and Vibration 289 (2006) 148–170
JOURNAL OF SOUND AND VIBRATION
www.elsevier.com/locate/jsvi

A mode-based approach for the mid-frequency vibration analysis of coupled long- and short-wavelength structures

L. Ji*, B.R. Mace, R.J. Pinnington

Institute of Sound and Vibration Research, University of Southampton, Highfield, Southampton SO17 1BJ, UK

Received 25 September 2003; received in revised form 15 September 2004; accepted 1 February 2005
Available online 29 March 2005

Abstract

A mode-based approach is described for the mid-frequency vibration analysis of a complex structure built-up from a long-wavelength source and a short-wavelength receiver. The source and the receiver respectively have low and high modal densities and modal overlaps. Each substructure is described in terms of its uncoupled, free-interface natural modes. The interface forces and displacements are decomposed in terms of a set of interface basis functions. Enforcing equilibrium and continuity conditions along the interface hence yields an analytical solution for the vibration response of the built-up structure. Expressions for the frequency response of the source and the power transmitted to the receiver are found. The correlations between the modal properties of the source and the receiver along the interface are derived. These modify the dynamic stiffness matrix of the structure. The flexible receiver is seen to add effective mass and damping to the source. The modes of the short-wavelength receiver are then described statistically in terms of a simple standing wave model. This approximation avoids the need for a modal analysis of the receiver. The results are compared with those of other methods including fuzzy structure theory. Numerical and experimental examples for beam-stiffened plate models are presented.

1. Introduction

Vibrations of complex structures occur in many practical situations, such as in vehicles, aircraft structures, mechanical equipment, and so on. These structures are usually built-up from

*Corresponding author. Tel.: +44 23 8059 3605; fax: +44 23 8059 3190.
E-mail address: lj@isvr.soton.ac.uk (L. Ji).

0022-460X/$ - see front matter © 2005 Elsevier Ltd. All rights reserved.
doi:10.1016/j.jsv.2005.02.003

substructures joined together at their interfaces. The substructures often have quite different vibration properties due to differences in material and geometric properties, for example. Consequently the vibrations of the whole structure often involve both long- and short-wavelength deformations. A number of challenges arise for the dynamic analysis of such built-up structures, mainly caused by the limitations of low frequency, finite element (FE) modelling [1–3] and high frequency, statistic energy analysis (SEA) modelling [4–7]. The associated vibration problems are hence characterised as 'mid-frequency' issues [8].

This paper concerns one aspect of the problem, namely the interaction of a long-wavelength source substructure with a short-wavelength receiver substructure. The source will be referred to as being 'stiff', by which is meant that it typically has a relatively long wavelength, low modal density and modal overlap, while its properties are well-defined: it is amenable to finite element analysis (FEA). The receiver, on the other hand, will be referred to as being 'flexible'. It has a relatively short wavelength, high modal density and high modal overlap, while its properties might be uncertainly defined. It is a suitable subsystem in a SEA model. There is therefore a mismatch between the source and the receiver, both in terms their dynamic properties and in terms of suitable analysis methods.

A number of specialist methods have been developed to solve such mid-frequency vibration problems. They include the hybrid FEA and analytical impedance (locally reacting) method [9,10], the SEA/modal technique in Refs. [11,12] and the fuzzy structure theory [13,14], which is the limit where the dynamic mismatch is very strong. However, more research is required before generally accepted methodologies are fully developed for this mid-frequency region.

In this paper the procedure used begins with a free-interface Component Mode Synthesis (CMS) model of the system [15,16]. Each component is described in terms of its uncoupled, free-interface modes and coupled using basis functions defined on the interface, similar to the approach of Refs. [17,18].

Various model reduction methods have been developed to reduce the size of a numerical model of a system, e.g. the CMS modal couplings in Refs. [15,16], the general objective being to use solutions of these intermediate problems to allow low-cost predictions of the global response. The main principle is to decompose the systems into components and perform intermediate computations at the component level. The well-established CMS models include fixed-interface modes (usually with constraint modes), free-interface modes (usually with attachment modes), hybrid-interface modes and loaded interface [15,16,19].

However, these conventional CMS models usually involve nodal degrees of freedom (dofs) along the interface between two substructures, and hence can lead to very large system models if the interfaces are continuous. Several approaches have been proposed to reduce the number of the interface dofs, including the generalized-interface-dofs method [17], the interface-modes methods [20,21] and the characteristic-constraint-modes (CC-modes) method [22]. In Ref. [17], the component coupling conditions were treated as generalized kinematic (for displacement) or natural (for force) boundary conditions. For compatible and incompatible meshes and for nodal and integral formulations, boundary conditions on discretized models take the form of a finite number of constraints which can be treated through a direct elimination or the addition of Lagrange multipliers. The generalizations of the treatment of interface boundary conditions and component model reduction give a very general framework to analyse a wide range of new and existing CMS methods. However, it does not eliminate the risk of poor predictions linked to

locking of incompatible component models. In Refs. [20,21], a truncated basis of interface modes and the associated generalised coordinates are used in place of the large number of supplementary static modes in the coupling procedure. The interface modes are defined as the first few eigenmodes obtained from such a reduced eigenproblem that results by projecting the structure stiffness and mass matrices on the global constraint modes. This, therefore, raises a main disadvantage that the substructures are no longer independent as the interface modes depends on the whole structure. As a result, the methods using interface modes are not significantly more efficient than the traditional CMS methods for some cases, e.g. for a single computation of the frequencies and modes. In Ref. [22], the CC modes were obtained by performing an eigenanalysis of the partitions of the CMS mass and stiffness matrices that corresponding to the Craig–Bampton constraint modes. When the CC modes are truncated, a CMS model with a highly reduced number of dofs may be obtained. The calculation and selection of CC modes is essentially a secondary modal analysis which can possibly be expensive when a very large number of constraint modes are involved. In addition, the benefits are mostly limited to fixed-interface CMS models.

In this paper, a mode-based approach is described to analyse the vibration of a built-up system comprising both long- and short-wavelength components as shown in Fig. 1. A source substructure is attached to a receiver substructure through arbitrary continuous interfaces. Each component is described in terms of its uncoupled, free-interface modes. A set of interface basis functions is defined on the interface between the subsystems, giving associated generalised interface coordinates. The coupling is then made in the subspace of the interface basis. Emphasis is put on predicting the frequency response functions (FRFs) of the source when loaded by the receiver and the power transmitted to the receiver. This can then be used to define the input power in an SEA model of the receiver. In this paper the receiver substructure is, in the first instance, assumed to be known exactly. Then it is allowed to have uncertainties in its properties so that its modal behaviour is approximated statistically. The response of the structure is found and compared with those of other methods, i.e., the hybrid SEA/modal technique of Refs. [11,12] and the fuzzy theory of Refs. [13,14]. Finally, the performance of the mode-based approach is demonstrated by both numerical and experimental examples on beam-stiffened plate models.

This mode-based approach is intended to serve the following two purposes: first, it can substantially reduce the system degrees of freedom (dofs) so as to reduce the computational cost; secondly, it has the ability to couple subsystems of different form within the same system model,

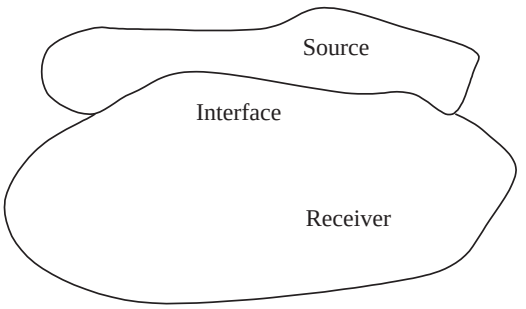

Fig. 1. A generic built-up structure.

the choice being determined by the local dynamic properties of the individual subsystem of interest.

The paper is organised as follows. In Section 2, modal analysis is briefly reviewed. Section 3 describes the mode-based approach. Approximations for the case of a stiff source and a flexible receiver are discussed in Section 4, and comparisons to those of Refs. [16–19] are made in Section 5. Sections 6 and 7 present numerical and experimental results.

2. Modal analysis of a continuous structure

In the approach described here predictions are based on the conventional modal analysis of both the source and the receiver substructures. Modal analysis theory is briefly reviewed in this section. The details can be found in many other works (e.g. Refs. [1,19]).

For a continuous undamped structure, the general form of the equation of motion is given by

$$\rho(\mathbf{x})\ddot{w}(\mathbf{x}) + L[w(\mathbf{x})] = F(\mathbf{x}), \tag{1}$$

where w is the displacement at a general location $\mathbf{x}$, $\rho(\mathbf{x})$ the mass density, L a differential (stiffness) operator of order $2p$ (where p is an integer) and F the applied force.

As a continuous function of position $\mathbf{x}$, the system response $w(\mathbf{x})$ can be expressed in terms of a complete set of orthogonal functions of space under the prescribed natural boundary conditions of the structure, i.e., the mode shape functions, as

$$w(\mathbf{x}) = \sum_n w_n \phi_n(\mathbf{x}), \tag{2}$$

where ϕ_n is the nth mode shape function of the structure and w_n is the associated generalized coordinate. The orthogonality property of ϕ_n gives

$$\int_V \rho(\mathbf{x})\phi_n^{\mathrm{T}}(\mathbf{x})\phi_{n'}(\mathbf{x})\,\mathrm{d}\mathbf{x} = 0, \quad n \neq n'. \tag{3}$$

Although theoretically an infinite number of modes are involved in any continuous structure, in practice the modal sums are usually truncated at a convenient finite number by a criterion of convergence. Combining Eqs. (1)–(3), the equation governing w_n is then given, in a matrix form, by

$$\mathbf{M}\ddot{\mathbf{w}}_\mathbf{n} + \mathbf{K}\mathbf{w}_\mathbf{n} = \mathbf{F}_\mathbf{n}, \tag{4}$$

where $\mathbf{M}$ and $\mathbf{K}$ are, respectively, the mass and stiffness matrices, and $\mathbf{F_n}$ is the generalized modal force vector. The (n, n')th elements of $\mathbf{M}$ and $\mathbf{K}$ are, respectively, given by

$$M_{nn'} = \int_V \rho(\mathbf{x})\phi_n^{\mathrm{T}}(\mathbf{x})\phi_{n'}(\mathbf{x})\,\mathrm{d}\mathbf{x}, \tag{5}$$

$$K_{nn'} = \int_V \phi_{n'}^{\mathrm{T}}(\mathbf{x})L[\phi_n(\mathbf{x})]\,\mathrm{d}\mathbf{x}. \tag{6}$$

Since ϕ_n satisfies both the partial differential equation (Eq. (1)) with no forcing and Eq. (3), it can be established that both $\mathbf{M}$ and $\mathbf{K}$ are diagonal [1,19]. In the context below, the nth diagonal

elements of $\mathbf{M}$ and $\mathbf{K}$ are simply represented by M_n and K_n, respectively. The nth element of $\mathbf{F_n}$ is given by

$$F_n = \int_V F(\mathbf{x})\phi_n(\mathbf{x})\,\mathrm{d}\mathbf{x}. \tag{7}$$

For time harmonic motion at frequency ω, Eq. (4) gives

$$\mathbf{w_n} = \mathbf{Y_n}\mathbf{F_n}, \tag{8}$$

where $\mathbf{Y_n}$ is a diagonal matrix, whose nth diagonal element corresponds to the dynamic receptance of the nth mode of the structure. Let damping be included by assigning a complex value to the stiffness as $K_n(1+\mathrm{j}\eta_n)$, where η_n is the damping loss factor associated with the nth mode of the structure. Y_n is then given by

$$Y_n = \frac{1}{M_n[\omega_n^2(1+\mathrm{j}\eta_n)-\omega^2]}, \tag{9}$$

where $\omega_n = \sqrt{K_n/M_n}$ is the nth natural frequency of the structure.

For convenience, $\phi_n(\mathbf{x})$ is usually mass-normalized in the form of $\Phi_n(\mathbf{x})$ such that

$$\int_V \rho(\mathbf{x})\Phi_n(\mathbf{x})\Phi_{n'}(\mathbf{x})\,\mathrm{d}\mathbf{x} = \delta_{nn'}, \tag{10}$$

where δ is kronecker function. M_n and K_n then become

$$M_n = 1, \quad K_n = \omega_n^2. \tag{11,12}$$

The above procedure is the conventional modal analysis for predicting the dynamic response of a continuous structure. In what follows, it is combined with an interface decomposition technique to predict the vibration response of the built-up structure shown in Fig. 1. Emphasis is then placed on the application where the source and the receiver are modally spare and dense, respectively.

3. Theory of the mode-based approach

In principle, the mode-based approach can be divided into the following steps: (1) both the source and the receiver substructures are described separately in terms of their uncoupled, free-interface modes, i.e., the mode shape functions when the individual substructures are separated from each other; (2) the interface forces and displacements are decomposed into a set of complete and orthogonal basis functions; (3) the equilibrium and continuity conditions are then enforced in terms of the interface basis functions. As a result, an analytical solution for dynamic response of the built-up structure can be determined in a simple manner. Moreover, the modal correlations and hence the dynamic interactions between the modes of the source and the receiver can be found. The detailed procedure is given below.

3.1. Modal analysis of the source substructure

The source substructure and its force loadings are shown in Fig. 2, where $F_e(\mathbf{x_s^e})$ and $F_I^s(\mathbf{x_s^I})$ represent the external and interface forces acting at the local coordinates $\mathbf{x_s^e}$ and $\mathbf{x_s^I}$ of the source,

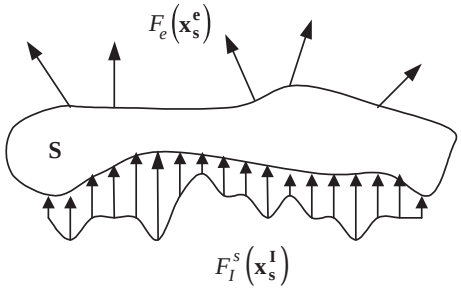

Fig. 2. The source sub-structure and its force loadings.

respectively. By the modal analysis theory described in Section 2, the displacement response w_s of the source at a general location $\mathbf{x_s}$, can be written as

$$w_s(\mathbf{x_s}) = \sum_n w_{s,n}\Phi_{s,n}(\mathbf{x_s}), \tag{13}$$

where $w_{s,n}$ is the nth generalized coordinate of the source, and $\Phi_{s,n}$ is its nth mass-normalized unloaded mode shape function, i.e.,

$$\int_{V_s} m_s(\mathbf{x_s})\Phi_n(\mathbf{x_s})\Phi_{n'}(\mathbf{x_s})\,\mathrm{d}\mathbf{x_s} = \delta_{nn'} \tag{14}$$

Here m_s is the mass distribution of the source substructure. Consequently, $w_{s,n}$ can be written, similar to Eq. (8), as

$$w_{s,n} = Y_{s,n}(f_{e,n} + f_{I,n}^s), \tag{15}$$

where $Y_{s,n}$ is the modal receptance of the nth natural mode of the uncoupled source, namely, the free-interface mode when the source is uncoupled with the receiver, and $f_{e,n}$ and $f_{I,n}^s$ are, respectively, the nth modal forces corresponding to $F_e(\mathbf{x_s^e})$ and $F_I^s(\mathbf{x_s^I})$. These terms are given by

$$Y_{s,n} = \frac{1}{\omega_{s,n}^2(1+\mathrm{j}\eta_{s,n}) - \omega^2}, \tag{16}$$

$$f_{e,n} = \int_{V_s^e} F_e(\mathbf{x_s^e})\Phi_{s,n}(\mathbf{x_s^e})\,\mathrm{d}\mathbf{x_s^e}, \tag{17}$$

$$f_{I,n}^s = \int_{V_s^I} F_I^s(\mathbf{x_s^I})\Phi_{s,n}(\mathbf{x_s^I})\,\mathrm{d}\mathbf{x_s^I}. \tag{18}$$

Here $\omega_{s,n}$ is the nth natural frequency of the uncoupled source (called the free-interface natural frequency), and V_s^e and V_s^I are, respectively, the region of the source over which the external and interface force loadings act. When a set of truncated mode shapes are used, Eq. (15) can then be written in matrix form as

$$\mathbf{w_{s,n}} = \mathbf{Y_{s,n}}(\mathbf{f_{e,n}} + \mathbf{f_{I,n}^s}), \tag{19}$$

where $\mathbf{w_{s,n}}$, $\mathbf{f_{e,n}}$ and $\mathbf{f^s_{I,n}}$ are column vectors composed of $w_{s,n}$, $f_{e,n}$ and $f^s_{I,n}$, respectively, while $\mathbf{Y_{s,n}}$ is a diagonal matrix whose nth diagonal element is $Y_{s,n}$. Substituting Eq. (15) into Eq. (13), the dynamic response of the source substructure can then be expressed in terms of its uncoupled, free-interface modes.

3.2. Modal analysis of the receiver substructure

The same analytical procedure can be applied to the receiver substructure shown in Fig. 3, where $F^r_I(\mathbf{x^I_r})$ is the interface force applied at the local coordinate $\mathbf{x^I_r}$.

Let the displacement w_r at a general location $\mathbf{x_r}$ of the receiver be expressed as

$$w_r(\mathbf{x_r}) = \sum_m w_{r,m}\Psi_{r,m}(\mathbf{x_r}), \tag{20}$$

where $w_{r,m}$ is the mth generalized coordinate of the receiver, and $\Psi_{r,m}$ is the mth uncoupled, free-interface mode in form of

$$\int_{V_r} m_r(\mathbf{x_r})\Psi_{r,m}(\mathbf{x_r})\Psi_{r,m'}(\mathbf{x_r})\,\mathrm{d}\mathbf{x_r} = \delta_{mm'}. \tag{21}$$

Here m_r is the mass distribution of the receiver. Following the same lines as in Section 3.1, the modal amplitudes of the receiver can be written as

$$\mathbf{w_{r,m}} = \mathbf{Y_{r,m}}\mathbf{f^r_{I,m}}, \tag{22}$$

where the subscript r denotes the receiver and the symbols have the same meaning as those given in Eq. (19). They are determined by

$$Y_{r,m} = \frac{1}{\omega^2_{r,m}(1+\mathrm{j}\eta_{r,m}) - \omega^2}, \tag{23}$$

$$f^r_{I,m} = \int_{V^I_r} F^r_I(\mathbf{x^I_r})\Psi_{r,m}(\mathbf{x^I_r})\,\mathrm{d}\mathbf{x^I_r}, \tag{24}$$

where $\omega_{r,m}$ is the mth free-interface natural frequency of the receiver and V^I_r represents the region of the receiver occupied by the interface.

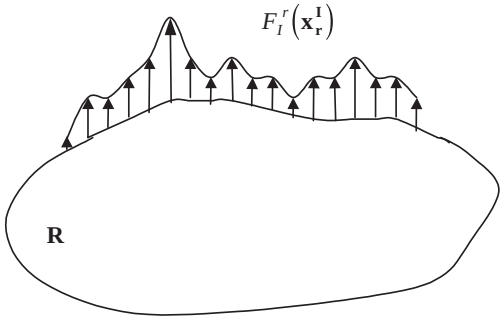

Fig. 3. The receiver sub-structure and its force loadings.

3.3. Decomposition of interface forces and displacements

Let $\mathbf{x_I}$ be the local coordinates of the interface, and $F_I(\mathbf{x_I})$ and $w_I(\mathbf{x_I})$ be, respectively, the interface forces and displacements. Now $F_I(\mathbf{x_I})$ and $w_I(\mathbf{x_I})$ are decomposed in terms of a set of complete, orthonormal basis functions, $X_k(\mathbf{x_I})$, as

$$F_I(\mathbf{x_I}) = \sum_k f_{I,k} X_{I,k}(\mathbf{x_I}), \tag{25}$$

$$w_I(\mathbf{x_I}) = \sum_k w_{I,k} X_{I,k}(\mathbf{x_I}), \tag{26}$$

where $f_{I,k}$ is the kth generalized interface force, $w_{I,k}$ is kth generalized interface coordinate, and since $X_k(\mathbf{x_I})$ is orthonormal, it exists that

$$\int_{V_I} X_{I,k}(\mathbf{x_I}) X_{I,k'}(\mathbf{x_I})\, \mathrm{d}\mathbf{x_I} = \delta_{kk'}. \tag{27}$$

From Eqs. (26) and (27), it is seen that the physical coupling dofs of the built-up structure have been transformed into generalized coupling dofs. Such approaches can reduce the number of coupling dofs involved in the calculation if a suitable set of basis functions is selected and truncated. Similar techniques have been described elsewhere, e.g., in Refs. [17,18].

3.4. Dynamic response of the built-up structure

Now truncate the set of basis functions to a convenient finite number. The force equilibrium and displacement compatibility conditions can then be enforced approximately, at least, along the interface in a simple manner.

The equilibrium and continuity conditions at the interface give

$$F_I(\mathbf{x_I}) = -F_I^s(\mathbf{x_I^s}) = F_I^r(\mathbf{x_I^r}), \tag{28}$$

$$w_I(\mathbf{x_I}) = w_s(\mathbf{x_I^s}) = w_r(\mathbf{x_I^r}). \tag{29}$$

The local coordinates $\mathbf{x_s^I}$, $\mathbf{x_r^I}$ and $\mathbf{x_I}$ can often be related by transformation matrices $\mathbf{T_s}$ and $\mathbf{T_r}$ [2,3,15,16] as

$$\mathbf{x_s^I} = \mathbf{T_s x_I}, \quad \mathbf{x_r^I} = \mathbf{T_r x_I}. \tag{30,31}$$

$\mathbf{T_s}$ and $\mathbf{T_r}$ are both orthogonal so that $\mathbf{T_s^T} = \mathbf{T_s^{-1}}$ and $\mathbf{T_r^T} = \mathbf{T_r^{-1}}$.

Combining Eqs. (18), (25) and (28), it yields,

$$f_{I,n}^s = -\sum_k f_{I,k} \int_{V_s^I} \Phi_{s,n}(\mathbf{x_s^I}) X_{I,k}(\mathbf{x_I})\, \mathrm{d}\mathbf{x_s^I}. \tag{32}$$

For truncated sets of source modes and interface basis functions, Eq. (32) can be expressed in a matrix form as

$$\mathbf{f_{I,n}^s} = -\boldsymbol{\alpha}_\mathbf{s} \mathbf{f_{I,k}}, \tag{33}$$

where $\mathbf{f_{I,k}}$ is a column vector of $f_{I,k}$, and $\boldsymbol{\alpha}_\mathbf{s}$ is a $n \times k$ matrix, given by

$$\alpha_{s,nk} = \int_{V_s^I} \Phi_{s,n}(\mathbf{x_s^I}) X_{I,k}(\mathbf{x_I})\, \mathrm{d}\mathbf{x_s^I}. \tag{34}$$

It is seen that $\boldsymbol{\alpha}_\mathbf{s}$ can be regarded as a modal correlation matrix in that its (n,k)th term indicates the correlation between the source mode $\Phi_{s,n}$ and the interface basis function $X_{I,k}$ along the interface. Eq. (19) then becomes

$$\mathbf{w_{s,n}} = \mathbf{Y_{s,n}}(\mathbf{f_{e,n}} - \boldsymbol{\alpha}_\mathbf{s}\mathbf{f_{I,k}}). \tag{35}$$

Similarly, for the receiver, combining Eqs. (24), (25) and (28), it gives

$$\mathbf{f_{I,m}^r} = \boldsymbol{\alpha}_\mathbf{r}\mathbf{f_{I,k}}, \tag{36}$$

where $\boldsymbol{\alpha}_\mathbf{r}$ is a $m \times k$ matrix representing the modal correlations between the receiver modes and the interface basis functions, given by

$$\alpha_{r,mk} = \int_{V_r^I} \Psi_{r,m}(\mathbf{x_r^I}) X_{I,k}(\mathbf{x_I})\, \mathrm{d}\mathbf{x_r^I}. \tag{37}$$

Eq. (22) then becomes

$$\mathbf{w_{r,m}} = \mathbf{Y_{r,m}}\boldsymbol{\alpha}_\mathbf{r}\mathbf{f_{I,k}}. \tag{38}$$

Continuity of displacements along the interface (Eqs. (13), (15), (20) and (29)) gives

$$\sum_n w_{s,n}\Phi_{s,n}(\mathbf{x_s^I}) = \sum_m w_{r,m}\Psi_{r,m}(\mathbf{x_r^I}) = \sum_k w_{I,k}X_{I,k}(\mathbf{x_I}). \tag{39}$$

Each side of Eq. (39) is multiplied by $X_{I,k}(\mathbf{x_I})$ and integrated along the interface V_I. From the orthogonality condition of Eq. (27), it follows that

$$\boldsymbol{\beta}_\mathbf{s}\mathbf{w_{s,n}} = \boldsymbol{\beta}_\mathbf{r}\mathbf{w_{r,m}} = \mathbf{w_{I,k}}, \tag{40}$$

where $\boldsymbol{\beta}_\mathbf{s}$ is a $k \times n$ matrix and $\boldsymbol{\beta}_\mathbf{r}$ is a $k \times m$ matrix given by

$$\beta_{s,kn} = \int_{V_I} X_{I,k}(\mathbf{x_I})\Phi_{s,n}(\mathbf{x_s^I})\, \mathrm{d}\mathbf{x_I}, \tag{41}$$

$$\beta_{r,km} = \int_{V_I} X_{I,k}(\mathbf{x_I})\Psi_{r,m}(\mathbf{x_r^I})\, \mathrm{d}\mathbf{x_I}. \tag{42}$$

Comparing Eqs. (41) and (42) with Eqs. (34) and (37), it is seen that

$$\boldsymbol{\alpha}_\mathbf{s} = \boldsymbol{\beta}_\mathbf{s}^\mathrm{T}, \quad \boldsymbol{\alpha}_\mathbf{r} = \boldsymbol{\beta}_\mathbf{r}^\mathrm{T}. \tag{43,44}$$

Combining Eqs. (35), (38), (40) and (43)–(44), the interface forces and displacements in terms of generalized interface coordinates can be determined by

$$\mathbf{f_{I,k}} = [\mathbf{A_s} + \mathbf{A_r}]^{-1}\boldsymbol{\alpha}_\mathbf{s}^\mathrm{T}\mathbf{Y_{s,n}}\mathbf{f_{e,n}}, \tag{45}$$

$$\mathbf{w_{I,k}} = \mathbf{A_r}[\mathbf{A_s} + \mathbf{A_r}]^{-1}\boldsymbol{\alpha}_\mathbf{s}^\mathrm{T}\mathbf{Y_{s,n}}\mathbf{f_{e,n}}, \tag{46}$$

where

$$\mathbf{A_s} = \boldsymbol{\alpha}_\mathbf{s}^\mathrm{T}\mathbf{Y}_{\mathbf{s,n}}\boldsymbol{\alpha}_\mathbf{s}, \quad \mathbf{A_r} = \boldsymbol{\alpha}_\mathbf{r}^\mathrm{T}\mathbf{Y}_{\mathbf{r,m}}\boldsymbol{\alpha}_\mathbf{r}. \tag{47,48}$$

Physically, $\mathbf{A_s}$ and $\mathbf{A_r}$ provide the dynamic correlations between the source modes, the receiver modes and the interface basis functions. The (k,k')th entries of $\mathbf{A_s}$ and $\mathbf{A_r}$ can be respectively calculated as

$$A_{s,kk'} = \sum_n \alpha_{s,kn}\alpha_{s,k'n}Y_{s,n}, \tag{49}$$

$$A_{r,kk'} = \sum_m \alpha_{r,km}\alpha_{r,k'm}Y_{r,m}. \tag{50}$$

The (k,k')th element of $\mathbf{A_s}$ hence represents how the free-interface modal properties of the source collectively affect the coupling between the kth and k'th interface basis functions. Combining Eqs. (35) and (45), the modal amplitudes of the source can then be determined by

$$\mathbf{w_{s,n}} = \mathbf{Y_{s,n}}[\mathbf{I} - \boldsymbol{\alpha_s}(\mathbf{A_s} + \mathbf{A_r})^{-1}\boldsymbol{\alpha}_\mathbf{s}^\mathrm{T}\mathbf{Y_{s,n}}]\mathbf{f_{e,n}}. \tag{51}$$

Eq. (51) indicates that the modes of the source become coupled after the source substructure is connected with the receiver, and so are the modes of the receiver. Meanwhile, it implies that the loads applied by the receiver substructure have the effect of a dynamic modification to the modal properties of the source substructure.

Finally, the time-averaged power transmission from the source to the receiver can be expressed as

$$P_{tr} = \frac{1}{2}\,\mathrm{Re}\left\{\int_{V_I}[F_I(\mathbf{x_I})]^*\mathrm{j}\omega w_I(\mathbf{x_I})\,\mathrm{d}\mathbf{x_I}\right\} = \frac{1}{2}\,\mathrm{Re}\left\{\mathrm{j}\omega\sum_k w_{I,k}f_{I,k}^*\right\}. \tag{52}$$

One key issue of the approach proposed here is how to select the set of interface basis functions appropriately. Theoretically, the set of basis functions can be arbitrary, provided it is complete and orthogonal. In practice, given that the set of basis functions is truncated to a finite number, the choice should meet criteria of convenience, simplicity and accuracy, and should depend on the local dynamic properties of the source and receiver structures, as well as the coupling conditions between them. For example, when a stiff source structure is wholly attached to a large flexible receiver, which is the case in the beam/plate example considered later, the choice of the mode shape functions of the source, being a set of complete and orthogonal functions, is obviously a proper one. Other forms of basis functions may be also appropriate. For example, sinusoidal basis functions (i.e., space harmonic) might be a good choice: they are orthogonal, and might couple well into a wave interpretation of the flexible receiver, with the higher-order functions contributing little to the transmitted power.

3.4.1. A special case: a simple form of coupling

It is interesting to consider a special case when the source and the receiver free-interface mode shapes have the same spatial variations along the interface region and form a complete, orthogonal set, such that

$$X_{I,k}(\mathbf{x_I}) = \Phi_{s,k}(\mathbf{x_s^I}) = \Psi_{r,k}(\mathbf{x_r^I}). \tag{53}$$

In this case, Eqs. (34) and (37) give

$$\boldsymbol{\alpha}_{\mathbf{s}} = \boldsymbol{\alpha}_{\mathbf{r}} = \mathbf{I}. \tag{54}$$

The generalized interface forces and displacements can then be written as

$$f_{I,n} = \frac{Y_{s,n}}{Y_{s,n} + Y_{r,n}} f_{e,n}, \tag{55}$$

$$w_{I,n} = \frac{Y_{s,n} Y_{r,n}}{Y_{s,n} + Y_{r,n}} f_{e,n}. \tag{56}$$

Eqs. (55) and (56) imply that for each substructure, its vibration modes remain uncoupled after the substructures are connected with each other. Furthermore, the dynamic stiffness at the interface is merely the sum of the modal dynamic stiffnesses of the two substructures. In this sense, Eq. (53) can be regarded as the simplest form of coupling between a source and a receiver. Further analysis for this special coupling case can be found in Ref. [8].

3.5. The dynamic interactions between a stiff source and a flexible receiver

Eq. (51) gives the dynamic response of the source substructure when the dynamic contributions arising from the presence of the receiver are included. In this subsection the dynamic effects of a flexible receiver on a stiff source are considered, this being relevant to many practical built-up structures.

3.5.1. The modified dynamic modal stiffness matrix

Let $n = k$ so that $\boldsymbol{\alpha}_{\mathbf{s}}$ is a square matrix. Eq. (51) can then be written as

$$\mathbf{w}_{\mathbf{s,n}} = \mathbf{Y}_{\mathbf{s,n}}[\mathbf{I} - (\mathbf{Y}_{\mathbf{s,n}} + \mathbf{Y}^{\mathbf{I}}_{\mathbf{rs}})^{-1}\mathbf{Y}_{\mathbf{s,n}}]\mathbf{f}_{\mathbf{e,n}} = [\mathbf{Y}^{-1}_{\mathbf{s,n}} + (\mathbf{Y}^{\mathbf{I}}_{\mathbf{rs}})^{-1}]^{-1}\mathbf{f}_{\mathbf{e,n}}, \tag{57}$$

where $\mathbf{Y}^{\mathbf{I}}_{\mathbf{rs}}$ is given by

$$\mathbf{Y}^{\mathbf{I}}_{\mathbf{rs}} = (\boldsymbol{\alpha}_{\mathbf{r}}\boldsymbol{\alpha}_{\mathbf{s}}^{-1})^{\mathrm{T}}\mathbf{Y}_{\mathbf{r,m}}(\boldsymbol{\alpha}_{\mathbf{r}}\boldsymbol{\alpha}_{\mathbf{s}}^{-1}). \tag{58}$$

It is seen from Eq. (57) that $\mathbf{Y}^{\mathbf{I}}_{\mathbf{rs}}$ has the same units as the receiver modal receptance matrix $\mathbf{Y}_{\mathbf{r,m}}$. While $\mathbf{Y}^{-1}_{\mathbf{s,n}}$ is the dynamic modal stiffness matrix of the source before it is coupled with the receiver, $\mathbf{Y}^{-1}_{\mathbf{s,n}} + (\mathbf{Y}^{\mathbf{I}}_{\mathbf{rs}})^{-1}$ is the one after the source is coupled with the receiver. Therefore $(\mathbf{Y}^{\mathbf{I}}_{\mathbf{rs}})^{-1}$ is in effect a representative of the dynamic stiffness modification matrix induced to the source substructure by the presence of the receiver. Consequently the (n, n)th diagonal element of $(\mathbf{Y}^{\mathbf{I}}_{\mathbf{rs}})^{-1}$ may be regarded as the *direct* modification to the nth mode of the source, i.e., through the couplings between the nth source mode and the receiver modes across the interface, whereas the (n, n')th element (where $n \neq n'$) is the *indirect* modification to the nth mode of the source, i.e., through the couplings between n'th source mode and the receiver modes.

A perturbation relation can be developed from Eq. (57) by letting

$$\mathbf{Y} = \mathbf{Y}_{\mathbf{s,n}} + \mathbf{Y}^{\mathbf{I}}_{\mathbf{rs}}. \tag{59}$$

Eq. (59) can then be expressed in the form of perturbation as

$$\mathbf{Y} = \mathrm{diag}[\mathbf{Y}]\{\mathbf{I} + (\mathrm{diag}[\mathbf{Y}])^{-1}\delta[\mathbf{Y}]\}, \tag{60}$$

where diag[**Y**] is a diagonal matrix comprising the diagonal elements of **Y** while δ[**Y**] is a full matrix comprising the off-diagonal elements of **Y**, i.e., the 'perturbation' of **Y**. $\mathbf{Y}^{-1}$ can thus be simply calculated by using a power-series expansion [23–25], assuming such an expression converges.

Generally, the vibration of the source structure tends to be less affected by the receiver substructure as the flexibility of the receiver increases. Therefore, it is reasonable to suppose that the coupling between the modes of the source is generally not very strong when the attached receiver substructure is relatively very flexible. Consequently one may assume that $(\mathbf{Y}^{\mathbf{I}}_{\mathbf{rs}})^{-1}$ is diagonally dominant for a stiff source and flexible receiver. Under such circumstances, the dynamic response of the source (Eq. (57)) can be simply approximated from the diagonal elements only, as

$$w_{s,n} \approx \frac{Y_{s,n}}{1 + Y_{s,n}/Y^I_{rs,n}} f_{e,n}, \tag{61}$$

where $Y^I_{rs,n}$ is the nth diagonal element of $\mathbf{Y}^{\mathbf{I}}_{\mathbf{rs}}$, given by

$$Y^I_{rs,n} = \sum_m \alpha^2_{nm} Y_{r,m}. \tag{62}$$

Here α_{nm} is the (n,m)th element of matrix $\boldsymbol{\alpha}_{\mathbf{r}}\boldsymbol{\alpha}_{\mathbf{s}}^{-1}$. Eq. (61) indicates that under these circumstances, the perturbation matrix δ[**Y**] can be approximated as being zero.

3.5.2. Effective mass and effective loss factor

From Eq. (61), the dynamic modifications to a stiff source, arising from the presence of a very flexible receiver, can then be regarded as some effective mass and loss factor added to each mode of the source. Let Eq. (62) be re-expressed as

$$Y^I_{rs,n} = -p'_{n1} - \mathrm{j}p'_{n2}, \tag{63}$$

where both p'_{n1} and p'_{n2} are real. Combining Eqs. (23), (60), (62)–(63), it follows that

$$p'_{n1} = \sum_m \frac{\alpha^2_{nm}(\omega^2 - \omega^2_{r,m})}{(\omega^2_{r,m} - \omega^2)^2 + (\omega^2_{r,m}\eta_{r,m})^2}, \tag{64}$$

$$p'_{n2} = \sum_m \frac{\alpha^2_{nm}\omega^2_{r,m}\eta_{r,m}}{(\omega^2_{r,m} - \omega^2)^2 + (\omega^2_{r,m}\eta_{r,m})^2}. \tag{65}$$

Substituting Eqs. (16), (63)–(65) into Eq. (61), gives

$$w_{s,n} \approx \frac{1}{\omega^2_{s,n}[1 + \mathrm{j}(\eta_{s,n} + \eta_n)] - (1 + m_n)\omega^2} f_{e,n}, \tag{66}$$

where

$$m_n = \frac{1}{\omega^2}\frac{p'_{n1}}{p'^2_{n1} + p'^2_{n2}}, \quad \eta_n = \frac{1}{\omega^2_{s,n}}\frac{p'_{n2}}{p'^2_{n1} + p'^2_{n2}}. \tag{67,68}$$

The dynamic modifications to the source by the receiver can then be interpreted as an effective loss factor η_n and an effective non-dimensional mass m_n being added to each mode of the source. Eq. (64) shows that m_n can be either positive or negative, depending on the relation between ω and

$\omega_{r,m}$: when $\omega < \omega_{r,m}$ (e.g. the mass-controlled region of the receiver), m_n is positive and the receiver adds mass to the source modes; else when $\omega > \omega_{r,m}$ (stiffness-controlled region), p'_{n1} is negative and the receiver adds stiffness to the source.

Note that these induced mass and loss factor are frequency-dependent quantities in this interpretation. As far as the response of the source is concerned, only the influences of m_n and η_n at $\omega \approx \omega_{s,n}$ are really important since the mass and damping effects are only important at the resonances.

4. Approximation of the receiving structure

The above procedure requires that both the source and the receiver substructures are defined precisely, i.e., in terms of their uncoupled, free-interface modes. However, as frequency increases, it becomes increasingly difficult, or even impossible, to give such a deterministic description for very flexible substructures due to the large number of modes involved and uncertainties in the geometric and material properties or the boundary conditions. It is desirable, therefore, to accommodate substructures whose dynamic properties are not known exactly.

4.1. Approximation of a short-wavelength structure

A short-wavelength structure tends to have relatively high mode count and modal overlap. Two main issues, concerning its modal analysis, arise [1,11,12]: first, the computational cost of full FEA is generally prohibitive, due to the large number of dof that may be required; and secondly, the system response becomes increasingly sensitive to geometrical imperfections as the wavelength of the response decreases so that even a highly detailed deterministic mathematical model based on the nominal system properties may not yield a reliable response prediction.

It is known from Ref. [1] that at frequencies higher compared with the fundamental natural frequency, then, as the modal overlap increases, the vibration response tends to be less sensitive to the detailed boundary conditions, size and shape of a structure, especially for points remote from the boundaries. Under such circumstances, the response of a uniform, wave-bearing substructure can be regarded as a sum of propagating waves which are spatially sinusoidal in nature. Consequently the response can locally be written as the superposition of a set of sinusoidal functions. In this case, therefore, instead of an exact description, the short-wavelength structure can be approximated in an asymptotic (or statistical) way, e.g. as a simple standing wave model with the modal density of the substructure giving an indication of the number of natural frequencies in a frequency band. Close to a boundary, where evanescent waves may exist, or where secular effects can persist over a wide frequency range, there are other problems associated with correlations of the mode shapes of successive modes [26]. However, these are separate issues and will not be discussed here.

4.2. Response approximation of a stiff source/flexible receiver system

In the built-up structure shown in Fig. 1, the source substructure is assumed to be well-defined with a low mode-count and long wavelength, while the receiver substructure is relatively much

more flexible with a high mode-count and short wavelength. Given a statistical approximation of the flexible receiver, the mode-based approach can then be used to estimate the broad features of the vibration response of the structure in a simple manner. These features include deterministic detail from the source but only statistical information (e.g. modal density) of the receiver.

When the receiver is approximated by a simple standing wave system, the modes can be estimated based on the wavenumber and the modal density of the substructure especially in a frequency average sense. Given a wavenumber k, the mode shape of a particular mode of the receiver, in this standing wave approximation, is proportional to

$$\Psi'_{r,m}(\mathbf{x_r}) \sim \prod_{\kappa} \sin(k_\kappa x_{r,\kappa} + \theta_{r,\kappa}), \tag{69}$$

where κ is the number of the dimensions of the receiver structure (e.g. $\kappa = 2$ for a plate and $\kappa = 3$ for a volume), where $\sum_\kappa k_\kappa^2 = k^2$, and $\theta_{r,\kappa}$ are the phase angles of the associated components. The exact value of $\theta_{r,\kappa}$ tends to be of less importance as the wavelength of the receiver decreases. At high frequencies, $\theta_{r,\kappa}$ can be assumed to be random [27].

For a plate-like receiver structure, for example, its modes may be estimated as

$$\Psi'_{r,m}(\mathbf{x_r}) \approx \frac{1}{\sqrt{m_r(\mathbf{x_r})}} \prod_{\kappa} \sqrt{\frac{2}{L_{r,\kappa}}} \sin\left(\frac{m_\kappa \pi x_{r,\kappa}}{L_{r,\kappa}} + \theta_{r,\kappa}\right), \tag{70}$$

where $\kappa = 2$, and $m_r(\mathbf{x_r})$ is the mass distribution of the receiver at a general location $\mathbf{x_r}$. Consequently, the mth natural frequency is approximated by

$$\omega'_{r,m} \approx \sum_{\kappa} \sqrt{\frac{D_r}{m_r}} \left(\frac{m_\kappa \pi}{L_{r,\kappa}}\right)^2, \tag{71}$$

where D_r corresponds to the stiffness of the receiver. Strictly, all the above parameters should be defined statistically, and the response estimated by ensemble averaging. In practice, at higher frequencies where the modal overlap is high, this approach is not required.

Such a statistical receiver model can then be easily incorporated into the mode-based procedure to estimate both the dynamic response of the source and the power transmitted to the receiver. Provided a sufficient number of assumed receiver modes is involved, the receiver modal overlap is large enough, and the interfaces are located far enough from the boundaries, the results can quite accurately represent the broad features of the vibration response of the coupled system, especially in a frequency average sense.

4.3. The mean-square response approximation of the receiver

From the power transmitted to the receiver, the total energy level of the receiver, when time and frequency averaged, can then be estimated from conservation of energy [1] as

$$E_r = \frac{P_{tr}}{\eta_r \omega}. \tag{72}$$

In the above equation it is assumed [1,4,5] that (1) the kinetic energy and the potential energy, when time averaged, are equal; (2) a sufficient number of modes of the receiver subsystem are resonant within the frequency band of excitation, and (3) the coupling is conservative.

The mean square velocity response of the receiver averaged over time, frequency and space, is thus given approximately by

$$\langle \overline{v_r^2} \rangle = \frac{E_r}{M_r} = \frac{P_{tr}}{\eta_r \omega M_r}, \tag{73}$$

where M_r is the total mass of the receiver.

5. Discussion

From the above analysis, it is seen that the mode-based approach can provide either an exact solution of the built-up structure when the dynamics of both the source and the receiver are exactly known, or an approximate one by involving a statistical model of the receiver modes, perhaps by using a standing wave approximation. This procedure is similar to that described in Refs. [11,12] in that the solution consists of a deterministic model of the long-wavelength (global) response and a statistical model of the short-wavelength (local) response.

The analysis also reveals that the dynamic interaction between source and receiver can be regarded as the receiver adding effective mass and damping to the source. These conclusions are in line with those obtained the hybrid SEA/modal technique [11,12] and fuzzy theory [13,14]. The detailed comparisons are given below.

5.1. Effective mass and damping induced by a 'fuzzy-like' receiver

Suppose that the receiver structure is very much more flexible than the source and has a high modal overlap such that it behaves as a set of fuzzy attachments to the source. In Ref. [16], the following approximate relations are taken to hold:

$$\mathrm{Re}\left\{\sum_m Y_{r,m}\right\} = \sum_m \frac{\omega_{r,m}^2 - \omega^2}{(\omega_{r,m}^2 - \omega^2)^2 + (\omega_{r,m}^2 \eta_r)^2} \approx 0, \tag{74}$$

$$\mathrm{Im}\left\{\sum_m Y_{r,m}\right\} = \sum_m \frac{-\omega_{r,m}^2 \eta_r}{(\omega_{r,m}^2 - \omega^2)^2 + (\omega_{r,m}^2 \eta_r)^2} \approx -\frac{\pi n_r}{2\omega}, \tag{75}$$

where n_r is the modal density of the receiver. If it is assumed that the receiver mode shapes over the interface are independent of their mode orders, at least over the restricted range of resonant modes [16], the term α_{nm}^2 in Eq. (62) may be approximated by its expectation as

$$\alpha_n^2 \approx E[\alpha_{nm}^2]. \tag{76}$$

Substituting Eqs. (74)–(76) into Eqs. (64) and (65), yields

$$p'_{n1} \approx 0, \quad p'_{n2} \approx \frac{\pi n_r}{2\omega} \alpha_n^2. \tag{77,78}$$

Consequently Eqs. (67) and (68) give

$$m'_n \approx 0, \tag{79}$$

$$\eta'_n \approx \frac{1}{\omega_{s,n}^2} \frac{2}{\pi n_r} \frac{\omega}{\alpha_n^2}. \tag{80}$$

Thus the effect of the very flexible, fuzzy-like receiver is to add damping to each mode of the source. Also the induced effective damping is independent of the internal damping of the receiver substructure.

The same conclusions can also be arrived at by a procedure similar to that used in Ref. [13]. The natural frequencies of a fuzzy receiver are closely spaced such that two adjacent natural frequencies lie well within each other's noise bandwidth such that

$$\omega_{r,m+1} - \omega_{r,m} \ll \frac{\pi}{2} \eta_r \omega_{r,m}. \tag{81}$$

Here the noise-bandwidth $\pi\eta_r\omega_{r,m}/2$ is used instead of the half-power bandwidth $\eta_r\omega_{r,m}$ used in Ref. [13]. This is because, when frequency averaged, it is the noise bandwidth that determines the response. In this case, Eqs. (64) and (65) yield the following approximations

$$p'_{n1} \approx 0, \quad p'_{n2} \approx \sum_m \frac{\alpha_{nm}^2}{\omega_{r,m}^2 \eta_r}. \tag{82,83}$$

By combining with Eq. (76), Eq. (82) can be written as

$$p'_{n2} \approx \alpha_n^2 \sum_m \frac{1}{\omega_{r,m}^2 \eta_r} \approx \alpha_n^2 N_r(\omega) E\left[\frac{1}{\omega_{r,m}^2 \eta_r}\right], \tag{84}$$

where $N_r(\omega)$ is the number of modes of the receiver resonating within the frequency range of $\omega \pm \pi\omega\eta/4$, and $E[1/\omega_{r,m}^2\eta_r]$ represents the mean value of $1/\omega_{r,m}^2\eta_r$ within that band. When the modal density of the receiver n_r varies little over the narrow frequency band, $N_r(\omega)$ is given approximately by

$$N_r(\omega) \approx \int_{\omega-\pi\eta_r\omega/4}^{\omega+\pi\eta_r\omega/4} n_r \, \mathrm{d}\omega \approx \frac{\pi}{2} \eta_r \omega n_r. \tag{85}$$

Let $E[1/\omega_{r,m}^2\eta_r]$ be approximated by

$$E\left[\frac{1}{\omega_{r,m}^2 \eta_r}\right] \approx \frac{1}{\eta_r \omega^2}. \tag{86}$$

Eq. (84) then becomes

$$p'_{n2} \approx \frac{\pi n_r}{2\omega} \alpha_n^2. \tag{87}$$

It is seen that Eqs. (82) and (87), which follow from fuzzy structure theory, are the same as those reached by the current approach in Eqs. (77)–(78) in the 'fuzzy' limit. Consequently, the same approximations for the effective damping and mass can be made as given in Eqs. (79) and (80), though different approximations are involved. However, this may raise an issue on how to estimate α_n^2 (Eq. (76)) appropriately.

6. Numerical examples

In this section numerical examples are presented for the beam-stiffened plate model shown in Fig. 4. The beam and the plate have a large dynamic mismatch. The system material is perspex with a Young's modulus of $4.4 \times 10^9\,\mathrm{N/m^2}$, a density of $1152\,\mathrm{kg/m^3}$, a material loss factor of 0.05 and a Poisson's ratio of 0.38. Both the beam and the rectangular plate are simply supported. The beam dimensions are 2 m long, 0.059 m wide and 0.068 m high. The plate dimensions are 2 m long (in the x-direction), 0.9 m wide (in the y-direction) and 0.005 m thick. In this case, the wavenumber ratio between the plate and the beam is $k_p/k_b = 3.5$. The interface locations are defined as: $x_1 = 0.03\,\mathrm{m}$, $y_1 = 0.3\,\mathrm{m}$ and $\theta = 10^\circ$. The beam is excited by a point force applied at $\xi = 0.73\,\mathrm{m}$. It is assumed that there are only translational couplings within the system.

Predictions are made first on the input mobility of the beam at the driving point when the beam is not joined to the plate by the conventional modal analysis procedure, and then on the input mobility of the beam and the power transmitted to the plate when the beam is coupled to the plate by the mode-based approach. Results are compared to those obtained by using the FRF-based sub-structuring method. (In the FRF method, input and transfer FRFs for both beam and plate are calculated as a sum of modal contributions. These result in large FRF matrices for continuous interfaces. Equilibrium and continuity boundary conditions are then applied at the discrete coupling points along the interface. The method is exact except for the approximation of the continuous line of coupling by many discrete points. Details are given in Ref. [8]). In all the calculations, the first 20 modes of the beam and the first 2000 modes of the plate are involved. For the mode-based approach the interface is decomposed into a set of beam modes (i.e., being the set of interface basis functions), while for the FRF-based method the interface is simulated by discrete point couplings spaced no more than a quarter wavelength of the plate apart [8]. For example, at 1000 Hz, the plate wavelength is about 0.138 m so that at least 58 coupling points are required at this frequency.

The results are shown in Figs. 5 and 6. The mode-based and the FRF-based sub-structuring methods provide almost exactly the same results, but the computational cost of the former is only about 3% of that of the latter. The reason is that the number of interface dofs has been substantially reduced. For example, the number of dofs in the FRF-based method, which depends on the plate wavelength, requires at least 58 coupling dofs at 1000 Hz, while the mode-based approach only uses 20, the number of beam modes retained. This advantage becomes more significant as frequency increases because the plate wavelength decreases.

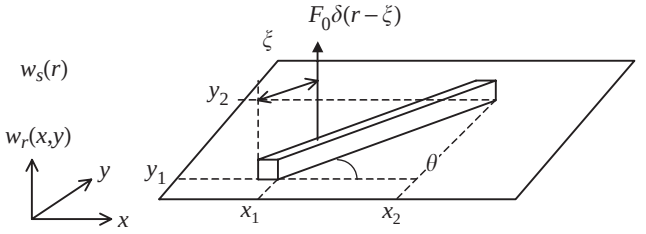

Fig. 4. The beam-stiffened plate.

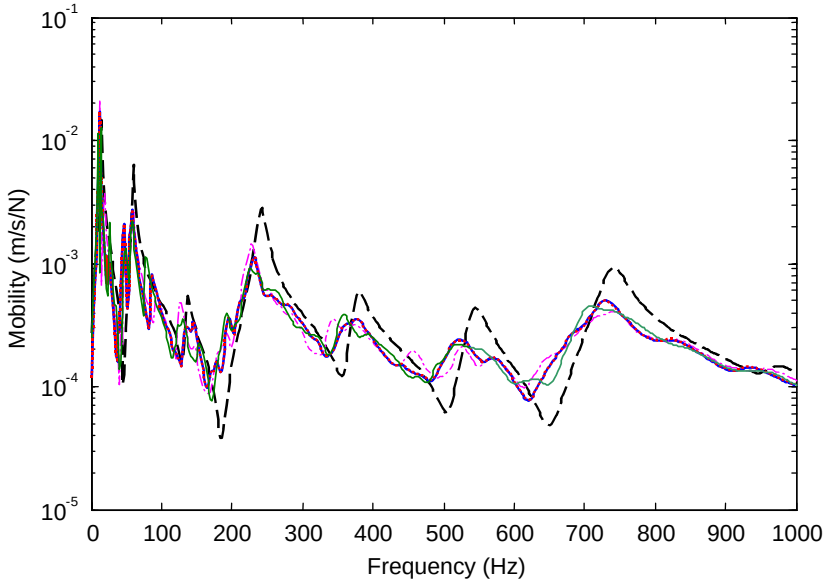

Fig. 5. Point mobility of the beam at the driving point: before coupling to the plate — —; after coupling to the original plate (——, mode-based approach; ....., FRF-based sub-structuring method); after coupling to the extended plate (——, mode-based approach), after coupling to the rotated plate (–·–·–, mode-based approach).

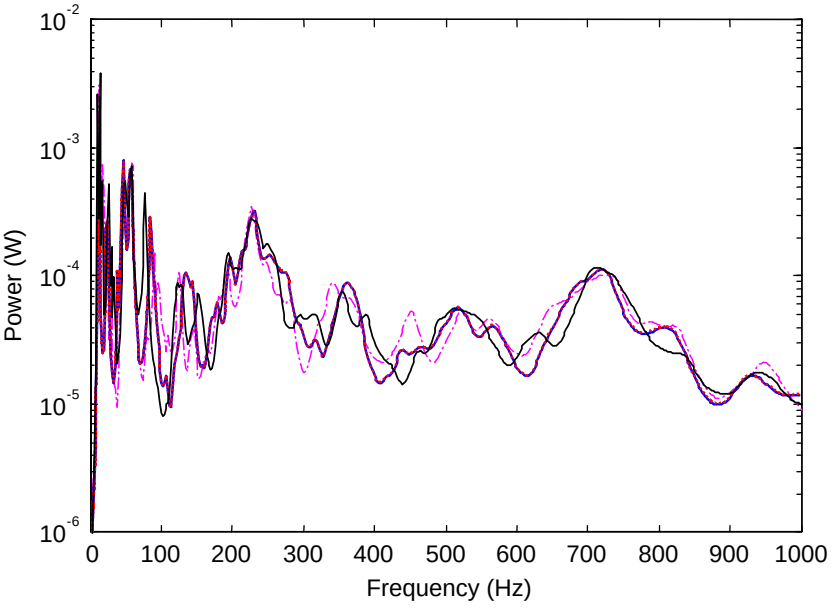

Fig. 6. Power transmitted from the beam to the plate: to the original plate (——, mode-based approach; ....., FRF-based sub-structuring method); to the extended plate (——, mode-based approach), to the rotated plate (–·–·–, mode-based approach.

Figs. 5 and 6 also show the results of the beam-stiffened plate model when either the plate is rotated such that the attachment angle θ is changed from 10° to 15°, or the beam is attached to a larger plate of dimension $2.5\,\mathrm{m} \times 1.2\,\mathrm{m}$. It is seen that for both cases, the main 'peaks' and 'troughs' of the response curves are largely controlled by the modal properties of the source beam. Only the small 'wrinkles' appearing in the response curves are sensitive to the dynamics of the plate receiver. These indicate that, as expected, the exact properties of the flexible receiver regarding boundary conditions, size and shape, are not important for estimating the broad features of the coupled response of the system.

Figs. 7 and 8 show the effective loss factor and mass induced to the first three modes of the beam by the plate, expressions being given in Eqs. (67) and (68). Two general trends can be seen: (1) the lower the order of the beam modes, the greater is the effective mass/damping added; (2) the effective damping for a given mode increases as frequency increases whereas the effective mass decreases with frequency. Therefore, as the wavelength of the plate gets shorter, its influence on the beam is mainly one of adding damping. The positions of the peaks of the effective mass and loss factor are determined by the modal properties of the plate, the coupling position on the plate and the mode shape functions of the beam. As the modal overlap of the plate increases, however, these peaks tend to smear out. In the case of infinite plate receiver, the effective mass and damping become smooth curves [8].

Fig. 8 also shows the results when the material loss factor of the plate itself is increased from 0.05 to 0.08. It is clear that the induced damping tends to be independent of the internal damping of the plate. This observation indicates that when the plate is very flexible and has high modal overlap, e.g., behaves like a set of fuzzy attachments to the beam, the effective loss factor can be

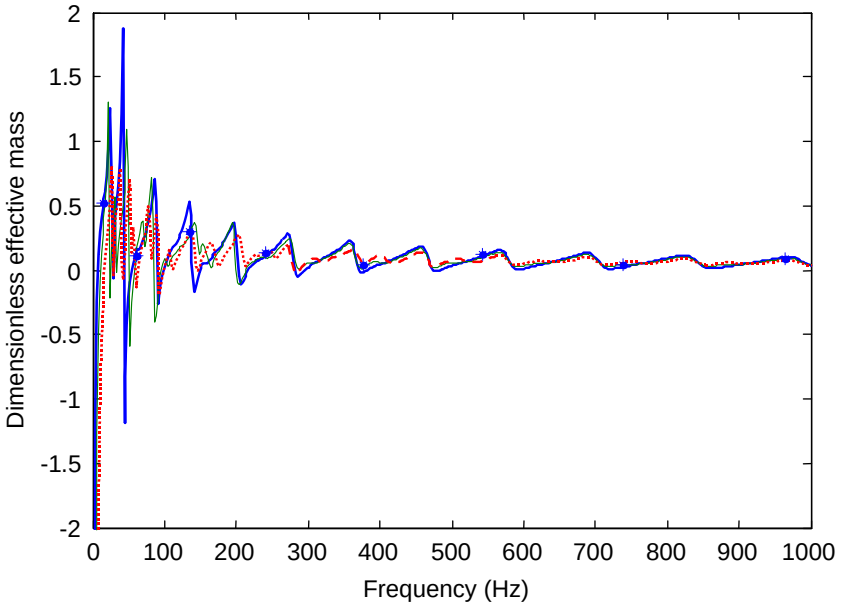

Fig. 7. Dimensionless effective mass induced to the first three modes of the beam by Eq. (73): (——, first; ——, second; — —, third).

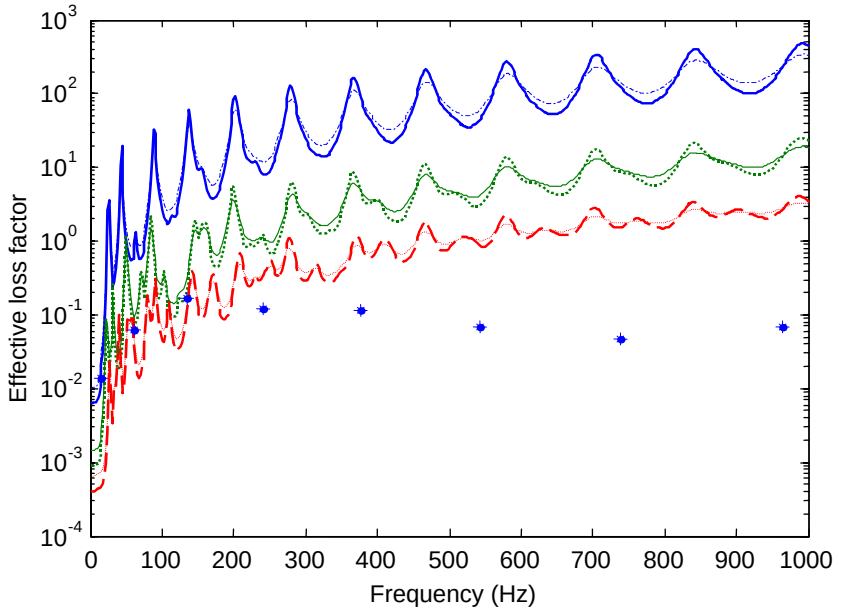

Fig. 8. Effective loss factor induced to the first three modes of the beam by Eq. (74): $\eta_p = 0.05$ (——, first; – – – –, second; — —, third); $\eta_p = 0.08$ (–·–·–, first; ——, second; ....., third).

reasonably treated as independent of the internal damping of the plate. Since the mass and damping effects are really only important at the beam resonances, it is suggested that one needs only consider the effects of m_n and η_n at $\omega \approx \omega_{b,n}$ in practice. Figs. 7 and 8 give the corresponding effective mass and damping results at the first eight natural frequencies of the beam.

7. Experimental investigations

Measurements were made on a freely suspended beam-stiffened plate. Both the beam and the plate are made of aluminium with a Young's modulus of $7.1 \times 10^9\,\mathrm{N/m^2}$, a density of $2700\,\mathrm{kg/m^3}$ and a Poisson's ratio of 0.33. The beam and plate dimensions are respectively $598 \times 12 \times 12\,\mathrm{mm^3}$ and $700 \times 500 \times 1\,\mathrm{mm^3}$, giving a wavenumber ratio of $k_p/k_b = 3.4$. The coupling locations lie along a line joining $(x_1, y_1) = (46, 319)\,\mathrm{mm}$ and $(x_2, y_2) = (618, 137)\,\mathrm{mm}$. Patches of constrained layer damping treatment were attached to the plate to increase its loss factor. Here η_p was estimated experimentally as 0.03 [8]. A random point force was applied to the beam at $\xi = 250\,\mathrm{mm}$. The point mobility of the beam and the surface velocity of the plate were measured directly. The power transmitted to the plate was then indirectly estimated by $P_{tr} \approx \eta_p \omega M_p \langle \overline{v_p^2} \rangle$ (Eq. (78)). This was done by measuring the velocity at many points on the plate and then estimating the spatially averaged mean square velocity.

The measured results are compared in Figs. 9 and 10 to those predicted for a free–free beam and a simple standing wave plate model. Further details can be found in Ref. [8]. It is seen that the agreement is generally good in the higher-frequency range but in the lower-frequency range

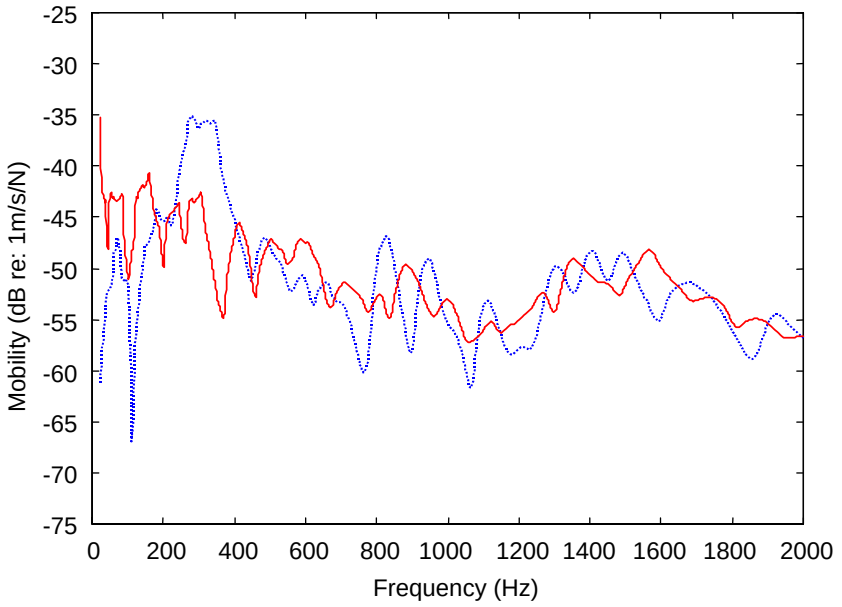

Fig. 9. Point mobility of the experimental beam model at the driving point (——, measured; ..... approximated by assuming a simple standing wave plate model).

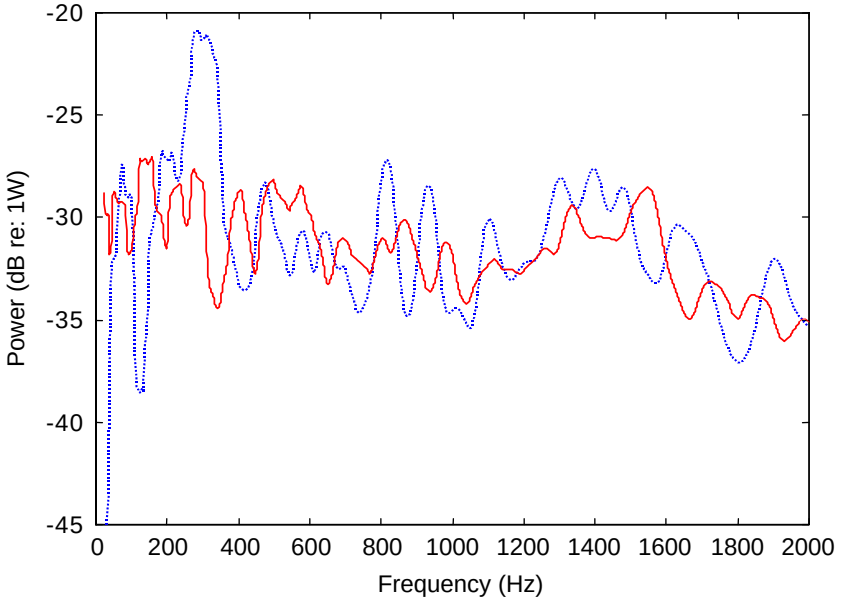

Fig. 10. Power transmitted to the experimental plate model (——, 'indirectly measured'; ..... approximated by assuming a simple standing wave plate model).

relatively large errors occur. This is because of the effects of the boundary conditions and the relatively long wavelength at low frequencies. As frequency increases, the plate modal overlap increases. The simple standing wave model becomes a more accurate representative of the behaviour of the system.

8. Concluding remarks

In this paper a mode-based approach for a system built-up from a long-wavelength source and a short-wavelength receiver was presented. In summary the steps are as follows:

(1) The source and the receiver substructures are described in terms of their uncoupled, free-interface modes.
(2) The interface force distribution between the source and the receiver is decomposed into a complete set of orthogonal interface basis functions.
(3) Equilibrium and continuity conditions at the interface are enforced in terms of the generalized interface coordinates.
(4) The response of the built-up structure and the power transmission within the system is then determined. The effect of the receiver is to load the source with a modal dynamic stiffness matrix. Expressions are derived for the effective mass and effective loss factor induced to each mode of the source.
(5) The mode-based approach is able to accommodate statistical models for the modes of the receiver. In particular, a standing wave approximation was described.
(6) The mode-based approach can be further extended to more general cases, where more than one type of wave motion may be involved, for example.

Comparisons were made with other methods, e.g., the hybrid SEA/modal technique in Refs. [11,12] and fuzzy structure theory in Refs. [13,14] when the built-up structure of interest is assumed to have a large dynamic mismatch. It was found that these approaches yield the same results in the 'fuzzy' limit.

Although the built-up structure considered only involves a stiff source and a flexible receiver, this mode-based approach can be further extended to structures comprising a number of substructures.

References

[1] L. Cremer, M. Heckl, E.E. Ungar, *Structure-Borne Sound*, second ed., Springer, Berlin, 1988.
[2] M. Petyt, *Introduction to Finite Element Vibration Analysis*, Cambridge University Press, Cambridge, MA, 1990.
[3] M. Lalanne, P. Berthier, J.D. Hagopian, *Mechanical Vibrations for Engineers*, Wiley, Chichester, 1984.
[4] F.J. Fahy, Statistical energy analysis: a critical overview, *Philosophical Transactions of the Royal Society of London A* 346 (1994) 431–447.
[5] R.H. Lyon, R.G. Dejong, *Theory and Application of Statistical Energy Analysis*, second ed., Butterworth-Heinemann, Boston, 1995.

[6] C.B. Burroughs, R.W. Fischer, F.R. Kern, An introduction to statistical energy analysis, *Journal of the Acoustical Society of America* 101 (1997) 1779–1789.
[7] J. Woodhouse, An introduction to statistical energy analysis of structural vibration, *Applied Acoustics* 14 (1981) 455–469.
[8] L. Ji, Mid-Frequency Vibration of Built-up Structures, PhD Thesis, ISVR, University of Southampton, 2003.
[9] R.M. Grice, R.J. Pinnington, A method for the vibration analysis of built-up structures—part I: introduction and analytical analysis of the plate stiffened beam, *Journal of Sound and Vibration* 230 (2000) 825–849.
[10] R.M. Grice, R.J. Pinnington, A method for the vibration analysis of built-up structures—part II: analysis of the plate stiffened beam using a combination of finite element analysis and analytical impedance, *Journal of Sound and Vibration* 230 (2000) 851–875.
[11] R.S. Langley, P.G. Bremner, A hybrid method for the vibration analysis of complex structural-acoustic systems, *Journal of the Acoustical Society of America* 105 (1999) 1657–1671.
[12] P.J. Shorter, B.K. Gardner, P.G. Bremner, A hybrid method for full spectrum noise and vibration prediction, *Fifth World Congress on Computational Mechanics*, July 7–12, Vienna, Austria, 2002.
[13] A.D. Pierce, V.W. Sparrow, D.A. Russell, Fundamental structural-acoustic idealisations for structures with fuzzy internals, *Transactions ASME Journal of Vibration and Acoustics* 117 (1995) 339–348.
[14] M. Strasberg, D. Feit, Vibration damping of large structures induced by attached small resonant structures, *Journal of the Acoustical Society of America* 99 (1996) 335–344.
[15] R.R. Craig Jr, A review of time-domain and frequency-domain component-mode synthesis methods, *International Journal of Analytical and Experimental Modal Analysis* 2 (1987) 59–72.
[16] R.R. Craig Jr, Substructure methods in vibration, *Journal of Vibrations and Acoustics* 117 (1995) 207–213.
[17] E. Balmes, Use of generalized interface degrees of freedom in component mode synthesis, *IMAC*, 1996, pp. 204–210.
[18] G. Kergoulay, E. Balmes, D. Clouteau, Model reduction for efficient FEM/BEM coupling, *ISMA*, 2000, p. 25.
[19] L. Meirovitch, *Principles and Techniques of Vibrations*, Prentice-Hall, Englewood Cliffs, NJ, 1997.
[20] F. Bourquin, Component modal synthesis and eigenvalues of second-order operators: discretization and algorithm, *Mathematical Modelling and Numerical Analysis* 26 (3) (1992) 385–423.
[21] D.-M. Tran, Component mode synthesis methods using interface modes. Application to structures with cyclic symmetry, *Computers and Structures* 79 (2001) 209–222.
[22] M.P. Castanier, Y.-C. Tan, C. Pierre, Characteristic constraint modes for component mode synthesis, *AIAA Journal* 39 (6) (2001) 1182–1187.
[23] B.R. Mace, P.J. Shorter, A local modal/perturbational method of estimating frequency response statistics of built-up structures with uncertain properties, *Journal of Sound and Vibration* 242 (2001) 793–811.
[24] J.H. Wilkinson, *The Algebraic Eigenvalue Problem*, Clarendon Press, Oxford, 1965.
[25] H.R. Schwarz, H. Rutishauser, E. Stiefel, *Numerical Analysis of Symmetric Matrices*, Prentice-Hall, Englewood Cliffs, NJ, 1973.
[26] M.W. Bonilha, F.J. Fahy, On the vibration field correlation of randomly excited flat plate structures—I: theory, *Journal of Sound and Vibration* 214 (3) (1998) 443–467.
[27] A.T. Moorhouse, B.M. Gibbs, Prediction of the structure-borne noise emission of machines: development of a methodology, *Journal of Sound and Vibration* 167 (1993) 223–237.